Am J Physiol Cell Physiol 319: C771–C780, 2020.
First published August 12, 2020; doi:10.1152/ajpcell.00279.2020.

METHODS IN CELL PHYSIOLOGY | *Making Cell Culture More Physiological*

Generation and optimization of highly pure motor neurons from human induced pluripotent stem cells via lentiviral delivery of transcription factors

Masood Sepehrimanesh and Baojin Ding

Department of Biology, University of Louisiana at Lafayette, Lafayette, Louisiana

Submitted 12 June 2020; accepted in final form 5 August 2020

Sepehrimanesh M, Ding B. Generation and optimization of highly pure motor neurons from human induced pluripotent stem cells via lentiviral delivery of transcription factors. *Am J Physiol Cell Physiol* 319: C771–C780, 2020. First published August 12, 2020; doi: 10.1152/ajpcell.00279.2020.—Generation of neurons from human induced pluripotent stem cells (hiPSCs) overcomes the limited access to human brain samples and greatly facilitates the progress of research in neurological diseases. However, it is still a challenge to generate a particular neuronal subtype with high purity and yield for determining the pathogenesis of diseased neurons using biochemical approaches. Motor neurons (MNs) are a specialized neuronal subtype responsible for governing both autonomic and volitional movement. Dysfunctions in MNs are implicated in a variety of movement diseases, such as amyotrophic lateral sclerosis (ALS). In this study, we generated functional MNs from human iPSCs via lentiviral delivery of transcription factors. Moreover, we optimized induction conditions by using different combinations of transcription factors and found that a single lentiviral vector expressing three factors [neurogenin-2 (NGN2), insulin gene enhancer 1 (ISL1), and LIM/homeobox 3 (LHX3)] is necessary and sufficient to induce iPSC-derived MNs (iPSC-MNs). These MNs robustly expressed general neuron markers [microtubule-associated protein 2 (MAP2), neurofilament protein (SMI-32), and tubulin β-3 class III (TUBB3)] and MN-specific markers [HB9 and choline acetyltransferase (ChAT)] and showed electrical maturation and firing of action potentials within 3 wk. This approach significantly improved the neuronal survival, yield, and purity, making it feasible to obtain abundant materials for biochemical studies in modeling movement diseases.

human induced pluripotent stem cells (hiPSCs); lentivirus; motor neurons; transcription factors

INTRODUCTION

Motor neurons (MNs) are a specialized neuronal subtype responsible for innervating musculature in the periphery and governing both autonomic and volitional movements (6). The process of MN specification in vivo consists of several sequential developmental stages, including neural induction in embryonic ectoderm, positioning along rostrocaudal and dorsoventral axes, and differentiation of specified neuronal precursors into postmitotic neuronal subtypes. In this developmental sequence, the interactions between intrinsic genes and extrinsic environmental clues ensure that numerous groups of genes should be turned on and off in response to extracellular signals in an elegant spatiotemporal manner (8, 23, 40). The combined actions of transcription factors, chemicals, and small molecules together with the bone morphogenic protein (BMP), Wingless and Int-1 (WNT), and fibroblast growth factor (FGF) signaling pathways have unique influences on neuronal identity and cell fate (2, 6, 23). Malfunctions in MNs caused by either degeneration or dysregulation are involved in a variety of movement diseases, such as amyotrophic lateral sclerosis (ALS), progressive muscular atrophy (PMA), spinal and bulbar muscular atrophy (SBMA), and dystonia (13, 16, 30, 42, 52). So far, there are no specific treatments available to cure these diseases because of unclear pathophysiological mechanisms. Generation of patient-specific MNs provides an unprecedented in vitro model system and greatly facilitates studies in deciphering the pathogenesis of these diseases (29, 33, 45).

MNs could be generated via direct conversion from adult fibroblasts by delivery of four transcription factors—neurogenin-2 (NEUROG2), insulin gene enhancer 1 (ISL1), LIM/homeobox 3 (LHX3), and sex-determining region Y (SRY)-box transcription factor 11 (Sox11)—with two lentiviruses (9, 33). However, the relative low purity and poor yield of directly converted MNs severely limit the applications that require a highly pure and large amount of cells, such as gene expression analysis by next-generation sequencing (NGS), and protein coimmunoprecipitation (Co-IP) and mass spectrometry (MS) analysis. As human induced pluripotent stem cells (hiPSCs) possess almost unlimited expansion capability, the approach of iPSC-based reprogramming and differentiation is feasible to generate a large number of human neurons for biochemical studies. Importantly, iPSCs could be prepared from a variety of readily available tissues such as skin and blood (49, 57). For instance, patient peripheral blood mononuclear cells (PBMCs) or skin fibroblasts could be used to generate hiPSCs by Yamanaka factors and then further induced into specific neuronal subtypes (55). These induced neurons have the same genetic background as the donors and could survive for a long time in cultured vessels to achieve fully functional maturation. These advantages make the iPSC-based approach a powerful tool in modeling neurological diseases (15, 18, 24).

Currently, there are several approaches to generate MNs from hiPSCs (Table 1). Small molecules such as growth factors and chemicals plus transcription factors are routinely used for neuronal induction. These factors either directly regulate genes or target signaling pathways that play critical roles in neurogenesis and differentiation. For example, GSK3β inhibitors such as CHIR99021 combine with the dual Sma and Mad proteins (SMAD) inhibitors, including SB 431542, a TGF-β receptor I kinase inhibitor, and LDN, a BMP type I receptor inhibitor, to induce neural progenitor cells (NPCs; 4, 17, 21, 31). In this way, it is crucial to use BMP inhibitors (Noggin and/or dorsomorphin), γ-secretase inhibitors (DAPT, tert-butyl

Correspondence: B. Ding (baojin.ding@louisiana.edu).

Table 1. *Approaches for generation of human iPSC-MNs*

Induction Factors*	Positive Markers	Characteristics†	Ref.
SB 431542, CHIR99021, dorsomorphin, and compound E	ChAT, HB9, SOX11, PAX6, nestin, OLIG2, TUJ1, neurofilament, and MAP2	MNs that form synaptic connections with bursting behavior, defined ion currents, and induced APs as well as calcium spikes (maturation time: 21 days)	(4)
SB 431542 and FGF2 or Noggin	HB9, ISL1, PAX6, SOX11, synapsin, OLIG2, and TUJ1	Rostrocaudal MNs that form synapses and give spontaneous postsynaptic currents (maturation time: 15 days)	(22)
SB 431542, Noggin, FGF2, and ROCK inhibitor	HB9, ISL1, PAX6, rosette markers, Nestin, PLZF, ZO1, OTX2, BF1, FOXG1, AP2, and PAX7	Spinal MNs and midbrain dopamine neurons (maturation time: 11 days)	(7)
SB 431542, dorsomorphin, BDNF, retinoic acid, and Smoothened agonist	ISL1/2, FOXP1, HOXA5, MAP2, TUJ1	Lateral motor column identity with a rostral phenotype that shows electrical spiking and activity (maturation time: 24 days)	(25)
RA and purmorphamine	ChAT, HB9, SMI-32, OLIG2, TUJ1	Caudoventralized spinal MNs with spontaneous and depolarization-induced action potentials (maturation time: 8 days)	(46)
SB 431542, CHIR99021, dorsomorphin, and RA	ChAT, HB9, SMI-32	Spinal cord MNs (maturation time: 24 days)	(17)
RA, Smoothened agonist, BDNF, GDNF, and DAPT	ChAT, HB9, ISL1, SMI-32, TUJ1	MNs that form physical and functional synapses with spontaneously occurring action potentials (maturation time: 32–38 days)	(20)
SB 431542, dorsomorphin, RA, smoothened agonist, GDNF, BDNF, and CNTF	ChAT, HB9, TUJ1	MNs with normal total neurite length, normal maximum neurite length, and normal number of nodes per MN (maturation time: 26–29 days)	(53)
SB 431542, dorsomorphin, RA, purmorphamine, cAMP, BDNF, GDNF, IGF-1	ChAT, HB9, ISL1	MNs that form end plate-like structures and induce clustering of acetylcholine receptors (maturation time: 42 days)	(48)
SB 431542, dorsomorphin, β-mercaptoethanol, insulin, CHIR99021, RA, purmorphamine, Compound E	ChAT, OLIG2, HOXB4, and SMI-32	Spinal cord neuron with spontaneous firing, containing glutamate receptors and voltage-dependent calcium channels (maturation time: 18 days)	(21)
SB 431542, LDN, CHIR99021, RA, Smoothened agonist, DAPT, BDNF, GDNF, and cAMP	ChAT, HB9, ISL1, MAP2, TUJ1, and synaptophysin	Spinal MNs with radial projection of neurites, defined electrophysiological characteristics, fast-activating, fast-inactivating inward Na^+ currents and large outward K^+ currents (maturation time: 12 days)	(31)
Purmorphamine, RA, dibutyryl-cAMP, BDNF, GDNF, and IGF-1	ChAT, HB9, ISL1, NGN2, OLIG2, LIM3, MNR2, FLAG, and DYKDDDDK tag	Spinal interneurons (maturation time: 28 days)	(3)
SB 431542, dorsomorphin, B18R, syn-TFs mRNAs of neurogenin and NeuroD families, forskolin, BDNF, GDNF, and NT-3	ChAT, HB9, and ISL1	Canonical MNs with stimulus-induced channel activities and electrical properties that exhibit action potential; this method decreases the differentiation time (maturation time: 10 days)	(19)
pLV-TRET-Ngn2–2A-Ngn1	ChAT, GLUT1, MAP2, and synapsin	Cortical neurons with functional synaptic activity and physiological action potential; this method has fewer medium changes (maturation time: 14 days)	(5)
NEUROG2, Sox11, ISL1, and LHX3	HB9, ChAT, TUBB3, MAP2, and synapsin	Low MNs with typical morphology and markers and high induction efficiency and purity (maturation time: 14 days)	(13, 51)

Chemicals include SB 431542 (a TGF-β receptor I kinase inhibitor), CHIR99021 [a glycogen synthase kinase-3 (GSK-3) inhibitor], dorsomorphin [an adenosine 5′-monophosphate-activated protein kinase (AMPK) inhibitor], compound E and DAPT (γ-secretase inhibitors), Y-27632 [a Rho-associated protein kinase (ROCK) inhibitor], retinoic acid (RA; a regulator of cell growth and differentiation), Smoothened agonist and purmorphamine [Hedgehog (Hh) signaling pathway activators], and forskolin (adenylyl cyclase activator that increases intracellular cAMP concentration as well as affects calcium currents and inhibits MAP kinase). Moreover, growth factors and small peptides comprise fibroblast growth factor 2 [FGF2, also referred to as basic fibroblast growth factor (bFGF), which stimulates neural precursor cell proliferation], Noggin [an inhibitor of bone morphogenic protein (BMP) signaling], brain-derived neurotrophic factor (BDNF; a canonical nerve growth factor), glial cell-derived neurotrophic factor [GDNF; supports the survival of dopaminergic and motor neurons (MNs)], ciliary neurotrophic factor (CNTF; promotes neurotransmitter synthesis and neurite outgrowth), insulin-like growth factor 1 (IGF-1), and neurotrophin-3 (NT-3; stimulates growth and differentiation of neurons and synapses). Finally, transcription factors enumerate as neurogenin-2 (NEUROG2 or NGN2), sex-determining region Y (SRY)-box transcription factor 11 (Sox11), insulin gene enhancer 1 (ISL1, or ISL LIM/homeobox 1), and LIM/homeobox 3 (LHX3; detailed functions are presented in Fig. 2*B*). ChAT, choline acetyltransferase; MAP2, microtubule-associated protein 2; SMI-32, neurofilament protein; TUJ1 or TUBB3, tubulin β-3 class III. HB9, homeobox gene 9; PAX6, paired box protein; PLZF, promyelocytic leukemia zinc finger; ZO-1, zona occludens protein; OTX2, orthodenticle homeobox 2; BF1, brain factor 1; FOXG1, forkhead box G1; PAX7, paired box protein 7; HOXA5, homeobox A5; Syn-TFs, synthetic transcription factors; DAPT, tert-butyl (2S)-2-[[(2S)-2-[[2-(3,5-difluorophenyl)acetyl]amino]propanoyl]amino]-2-phenylacetate. *Generation of human induced pluripotent stem cell (iPSC)-derived MNs (iPSC-MNs) can be done via chemicals, growth factors, small peptides, and transcription factors. †Maturation time is defined by different criteria in different studies.

(2S)-2-[[(2S)-2-[[2-(3,5-difluorophenyl)acetyl]amino]propanoyl] amino]-2-phenylacetate or compound E), antioxidants [cAMP or β-mercaptoethanol (β-ME)], and insulin-like growth factor 1 (IGF-1) or insulin to boost NPC proliferation. Then, retinoic acid (RA), purmorphamine, or Smoothened agonist can activate sonic hedgehog (SHH) signaling and induce choline acetyltransferase (ChAT)-positive MNs (3, 21, 31). The presence of brain-derived neurotrophic factor (BDNF), glial cell-derived neurotrophic factor (GDNF), ciliary neurotrophic factor (CNTF), or neurotrophin-3 (NT-3) in the culture medium is necessary to maintain the neuronal survival and promote neuronal maturation (20, 48, 51). Regardless of the extensive use of these small molecules, these methods have poor efficiency, produce clear heterogeneity in neuronal subtypes, and are time and cost consuming. Therefore, new methods of creating iPSC-derived MNs (iPSC-MNs) are being developed (Table 1). Lentiviral delivery of transcription factors is an alternative approach (51).

In this study, we generated functional mature MNs via hiPSC-based induction and differentiation. Human iPSCs were induced into NPCs and then transduced with a set of transcription factors as used in the direct conversion approach (13, 51). Moreover, we closely examined and compared the induction efficiency with different combinations of factors. We found that the transduction of NPCs with a single lentivirus coexpressing three factors (NEUROG2, ISL1, and LHX3) is necessary and sufficient to generate iPSC-MNs. Most importantly, by using a single lentiviral vector, the transduction efficiency was maximized and simultaneously the cell death was minimized. Our study provides an optimized approach to generate highly pure iPSC-MNs with very high yield, making it feasible to obtain abundant materials for biochemical studies in modeling movement diseases.

METHODS

Cell lines and culture conditions. Human embryonic kidney (HEK) 293T cells [American Type Culture Collection (ATCC) cat. no. CRL-11268, RRID:CVCL_1926] and human wild-type iPSCs (Coriell cat. no. GM23476, RRID:CVCL_T841) were purchased from ATCC and Coriell Institute for Medical Research, respectively. Human iPSCs were maintained in complete mTeSR1 medium (STEMCELL Technologies cat. no. 85850) on Matrigel (Corning cat. no. 356234)-coated dishes at 37°C and 5% CO_2, and the medium was replaced daily. As in previous reports (9, 51), the detailed medium recipes were as follows:

1) HEK medium (lentivirus preparation medium) consisted of DMEM (GIBCO) supplemented with 10% fetal bovine serum (FBS; Corning) and 1% penicillin-streptomycin (P/S; GIBCO).
2) iPSC medium (complete mTeSR1 medium) consisted of mTeSR1 basal medium supplemented with mTeSR1 supplement (STEMCELL Technologies) and 1% P/S.
3) KnockOut Serum Replacement (KOSR) medium consisted of KOSR (Thermo Fisher Scientific), 1% GlutaMax (GIBCO), 1% nonessential amino acid (NEAA; GIBCO), 50 μM β-mercaptoethanol (β-ME; GIBCO), and 1% P/S.
4) Neurosphere (NSP) medium consisted of DMEM/F-12 medium containing 1% N2 (Invitrogen), 1% GlutaMax, 1% NEAA, 1% P/S, 50 μM β-ME, 8 μg/mL heparin (STEMCELL Technologies), 20 ng/mL basic fibroblast growth factor (bFGF), and 20 ng/mL epidermal growth factor (EGF; PeproTech).
5) NPC medium consisted of DMEM/F-12 and neurobasal medium (1:1) containing 0.5% N2 (Invitrogen), 1% B27 (Invitrogen), 1% GlutaMax, 1% NEAA, 50 μM β-ME, 1% P/S, 10 ng/mL EGF, 10 ng/mL bFGF, and 1% P/S.
6) Neuronal maturation medium consisted of DMEM-F-12-neurobasal medium (2:2:1), 0.8% N2, 0.8% B27, and 1% P/S, supplemented with 5 mM forskolin (FSK; Sigma-Aldrich) and 10 ng/mL each of BDNF (PeproTech), GDNF (PeproTech), and neurotrophin-3 (NT-3; PeproTech).

Note that it is critical to freshly prepare a complete culture medium and use it up within 1 wk. A very old complete culture medium (>2 wk) may affect cell growth and even cause contamination.

Plasmids and virus production. As previously described (13, 33, 51), a third-generation lentiviral vector (pCSC-SP-PW-IRES-GFP) was used to express NEUROG2-IRES-GFP (*plasmid 1*), NEUROG2-IRES-GFP-T2A-Sox11 (*plasmid 2*, Addgene no. 90214), and ISL1-T2A-LHX3 (*plasmid 3*, Addgene no. 90215). The DNA sequence of NEUROG2-IRES in *plasmid 2* was subcloned into *plasmid 3* and constructed NEUROG2-IRES-ISL1-T2A-LHX3 (*plasmid 4*), in which three transcription factors are coexpressed in a single lentiviral vector (Fig. 2*A*). Replication-incompetent lentiviruses were produced in HEK293T cells, and viral supernatants were collected at 48 h and 72 h posttransfection. Viral supernatants were filtered through 0.45-μm syringe filters and titered as previously described (9, 12). Lentiviruses were stored at 4°C before cell transduction.

Note that high-quality supercoiled plasmid is critical to prepare lentivirus with good titer. The purity and the supercoiled conformation of plasmids could be examined by NanoDrop and running agarose gels as in a previous report (12).

NPC generation. NPCs were generated as previously reported (13, 56). Briefly, hiPSCs were cultured in mTeSR1 medium with 10 μM all-trans-retinoic acid (RA; Sigma) and 0.5 mM valproic acid (VPA; Sigma) on Matrigel-coated six-well plates for 7 days. iPSCs were then digested with Versene (Thermo Fisher Scientific) and gently pipetted into small clumps supplemented with 10 μM Y-27632 Rho-associated protein kinase (ROCK) inhibitor (STEMCELL Technologies). Cell clumps were aggregated in the KOSR medium for 4 days, followed by culturing in the NSP medium for another 1 wk. Neurospheres were then formed and dissociated into single cells by Accutase (Innovative Cell Technologies). NPCs were maintained and expanded on Matrigel-coated six-well plates in NPC medium. When cells reached ~90% confluence, NPCs were frozen in freezing medium (NPC medium supplemented with 10% DMSO) and kept in liquid nitrogen for long-term storage.

Note that all-trans-RA is light and temperature sensitive. Keep it from light during storage and performance. To maintain an effective concentration of chemicals, it is important to change the induction medium daily.

Neural differentiation. Neural differentiation was conducted as in previous reports (13, 51) with further modifications. For spontaneous differentiation, NPCs were plated onto Matrigel-coated plates at a density of 5×10^4 cells/cm^2 and cultured with neuronal maturation medium containing 5 mM FSK and 10 ng/mL each of BDNF, GDNF, and NT-3. The medium was half-changed every other day until analysis. For transcription factor-induced differentiation, NPCs were seeded onto Matrigel-coated plates at a density of 3×10^4 cells/cm^2 overnight and infected with lentiviruses expressing desired transcription factors. In this study, three different combinations of transcription factors were employed to generate iPSC neurons: *1*) NEUROG2 alone (N, *lentivirus 1*); *2*) NEUROG2, ISL1, LHX3, and Sox11 (N-S-I-L, *lentiviruses 2* and *3*); and *3*) NEUROG2, ISL1, and LHX3 (N-I-L, *lentivirus 4*; Fig. 2*A*). The multiplicity of infection (MOI) was about 2 for a single virus and 4 for the cocktail of two lentiviruses (1:1). The next day, the medium was replaced with a neuronal maturation medium containing 5 mM FSK and 10 ng/mL each of BDNF, GDNF, and NT-3. Neurons were then dissociated by Accutase at 5 days postinfection (dpi) and replated onto astrocyte-coated coverslips at a density of 1×10^3 cells/cm^2. Mouse astrocytes were isolated from *postnatal day 1* (P1) pups and cultured in DMEM with 15% FBS as reported (47). The medium was changed twice a week until analysis.

Note that at transduction, the proper NPC density (50–60% confluence) is critical to obtain high-yield iPSC-MNs. Too high and too low cell density at transduction will cause more cell death.

Immunostaining. Cultured cells at indicated time points were fixed with 4% paraformaldehyde (PFA) in phosphate-buffered saline (PBS) for 15 min at room temperature and then incubated in a blocking buffer [PBS containing 3% bovine serum albumin (BSA) and 0.2% Triton X-100] for 1 h for permeabilization and blocking. Cells were then incubated with primary antibodies in a blocking buffer at 4°C overnight, followed by washing and incubation with fluorophore-conjugated corresponding secondary antibodies. The primary antibodies used in this study were microtubule-associated protein 2 (MAP2, Abcam cat. no. ab5392, RRID: AB_2138153, 1:10,000; and Sigma-Aldrich cat. no. M4403, RRID: AB_477193, 1:500), tubulin β-3 class III (TUBB3, 1:2,000; Covance Research Products Inc. cat. no. MMS-435P, RRID:AB_2313773, and cat. no. PRB-435P-100, RRID:AB), HB9 (1:500; DSHB, cat. no. 81.5C10-c), ChAT (1:200, Millipore cat. no. AB144P, RRID: AB_2079751), vesicular glutamate transporter 1 [VGLUT1, 1:100; University of California, Davis/National Institutes of Health (NIH) NeuroMab Facility cat. no. 75-066, RRID:AB_2187693], VGLUT3 (1:100; University of California, Davis/NIH NeuroMab Facility cat. no. 75-073, RRID:AB_2187711), γ-aminobutyric acid (GABA, 1:1,000; Sigma-Al-

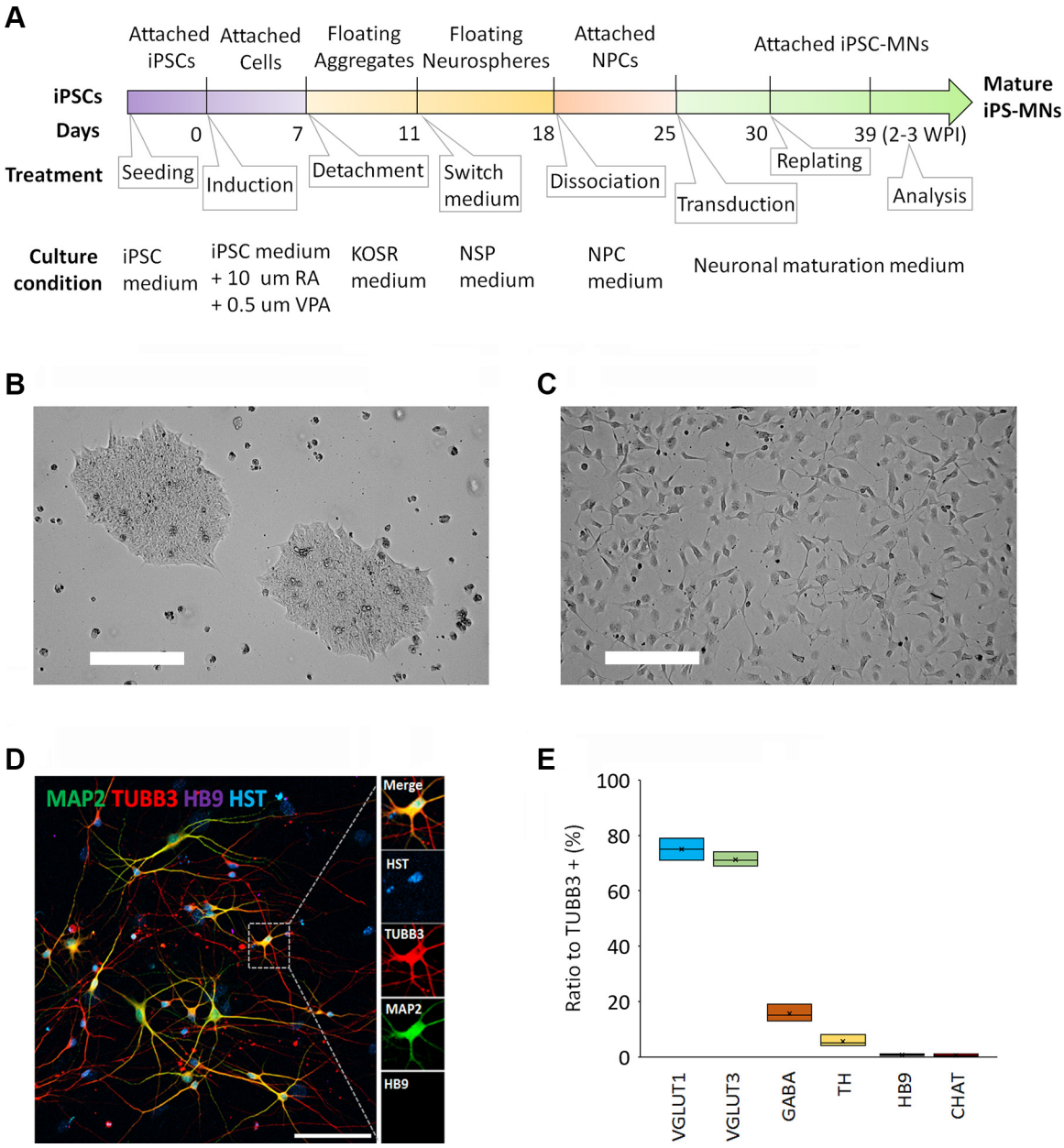

Fig. 1. Generation of human neurons from induced pluripotent stem cells (iPSCs). *A*: a schematic shows the process of the generation of human motor neurons (MNs) from iPSCs. The starting induction time was set as *day 0*. The age of iPSC-derived MNs (iPSC-MNs) was counted from lentiviral transduction. KOSR, KnockOut Serum Replacement; NPCs, neuronal progenitor cells; NSP, neurosphere; RA, retinoic acid; VPA, valproic acid; WPI, weeks post-viral infection. *B*: a representative phase contrast micrograph of human iPSCs. Scale bar, 200 μm. *C*: a representative phase contrast micrograph of NPCs. Scale bar, 200 μm. *D*: a confocal micrograph of spontaneously differentiated neurons from NPCs at 3 wk. Hoechst 33342 (HST)-stained nuclei. Scale bar, 100 μm. *E*: quantification of neuron identity shown as the ratios of specific markers to tubulin β-3 class III (TUBB3)+ cells. Number of neurons $n > 300$ from 3 biological replicates. ChAT, choline acetyltransferase; GABA, γ-aminobutyric acid; MAP2, microtubule-associated protein 2; TH, tyrosine hydroxylase; VGLUT1, vesicular glutamate transporter 1; VGLUT3, vesicular glutamate transporter 3.

drich cat. no. A2052, RRID:AB_477652), tyrosine hydroxylase (TH, 1:1,000; LifeSpan cat. no. LS-C149142-200, RRID:AB_11145263), and SMI-32 (1:5,000; BioLegend cat. no. 801701, RRID:AB_2564642). The secondary antibodies used in this study were purchased from Jackson ImmunoResearch Laboratories. They were Alexa Fluor (AF)488 anti-mouse (cat. no. 715-545-150, RRID:AB_2340846), AF594 anti-mouse (cat. no. 715-585-151, RRID:AB_2340855), AF647 anti-mouse (cat. no. 715-605-150, RRID:AB_2340862), AF488 anti-rabbit (cat. no. 711-545-152, RRID:AB_2313584), AF594 anti-rabbit (cat. no. 711-585-152, RRID:AB_2340621), AF647 anti-rabbit (cat. no. 711-605–152, RRID:AB_2492288), AF488 anti-chicken (cat. no. 703-545-155, RRID:AB_2340375), and AF594 anti-chicken (cat. no. 703-585-155, RRID:AB_2340377; 10, 11, 14, 33, 51). The nuclei were stained with Hoechst 33342 (HST, 1 μg/mL; Thermo Fisher Scientific).

Imaging and quantification. Living cells were visualized in culture plates with a CKX53 inverted microscope (Olympus). Immunostaining images were obtained with a Leica SP5 confocal microscope in the Microscopy Center at the University of Louisiana at Lafayette. ImageJ software (NIH) was used to quantify the neurons based on specific markers. An iPSC-induced neuron was defined by highly expressed neuron-specific markers TUBB3 and/or MAP2. An MN was defined by the robust expression of nuclear HB9 [also named motor neuron and pancreas homeobox 1 (MNX1)] at early developmental stages and/or high levels of ChAT in the soma at late mature stages. The purity of iPSC-differentiated MNs was calculated by the ratio of HB9+ cells to TUBB3+ cells at the early developmental stages and the ratio of ChAT+ cells to TUBB3+ cells at the late mature stages. The yield and the surviving neurons were counted on the basis of TUBB3 signals and normalized to the number of starting materials.

Neuronal survival assay. Induced neurons were replated onto astrocyte-coated 96-well plates at a cell density of 1×10^3 cells/cm^2 and cultured in neuronal maturation medium. The medium was changed twice a week until analysis with immunostaining at desired time points. The surviving neurons were counted on the basis of having typical neuronal morphology after immunostaining of TUBB3 and showing clear nuclei with HST staining. The number of neurons at the first week post-viral infection (WPI) was set as 100% and used for normalization of surviving neurons at 2 and 3 WPI. Three wells of neurons were examined under each condition at each time point.

Electrophysiology. Whole cell patch-clamp recordings were used to verify the neuronal electrophysiological maturation as in previous reports (13, 33) with minor modifications. Briefly, induced MNs were cultured on astrocyte-coated glass coverslips for 3 WPI and used for analysis. Cells were maintained at 30°C in a submersion chamber with Tyrode solution containing 150 mM NaCl, 4 mM KCl, 2 mM $MgCl_2$, 3 mM $CaCl_2$, 10 mM glucose, and 10 mM HEPES at pH 7.4 (adjusted with KOH) and 300 mOsm. The recording pipettes (~6–9 MΩ) were filled with an intracellular solution containing 0.2 mM EGTA, 130 mM K-gluconate, 6 mM KCl, 3 mM NaCl, 10 mM HEPES, 4 mM ATP-Mg, 0.4 mM GTP-Na, and 14 mM phosphocreatine-di (Tris) at pH 7.2 and 285 mOsm. Action potentials (APs) were recorded in current-clamp and elicited by a series of current injections ranging from −20 to 200 pA at 20-pA increments and 800 ms in duration. All current-clamp recordings were made at resting membrane potential or without any current injection. Data analysis was performed with Clampfit 10.3 software (Molecular Devices). The AP trace immediately above the threshold was used to determine the delay of the first spike as the length of time and the start of current steps to the peak of AP. The same AP trace was used to measure the AP threshold as the corresponding voltage when there was the sharpest change of the trace slope. The above-indicated AP trace was also measured to determine the maximum velocity of the rise and decay. AP frequency was obtained by dividing the maximum number of spikes during the current step protocol by the step time duration (800 ms).

Statistical analysis. Data are presented as means ± SE from at least three biological replicates. Statistical analysis was conducted by one-way analysis of variance and statistical significance was set at a P value of <0.05.

RESULTS

Human MNs cannot be obtained via spontaneous differentiation of iPSC-NPCs. To generate a large number of MNs with high purity, we tried the iPSC-based approach. As previously reported (13, 51), human iPSCs were first induced into NPCs by exposure to all-trans-RA and VPA in the culture medium (Fig. 1, *A–C*). NPCs were rapidly expanded with a population doubling time (PDT) of ~35 h. Human iPSC-derived NPCs could spontaneously differentiate into neurons if they are cultured in neuron maturation medium. We have systematically analyzed the neuronal identity with immunostaining of different markers in the third week, a time point at which most types of NPC-derived neurons reach the maturation stage (13, 51). Generic neuron markers including MAP2 and TUBB3 revealed that these spontaneously differentiated neurons are a mixture of different neuronal populations. They vary greatly in cellular morphology and soma size (Fig. 1*D*). MNs can be identified by robustly expressed nuclear HB9 at early stages and high levels of ChAT in the soma at late mature stages (1,

A

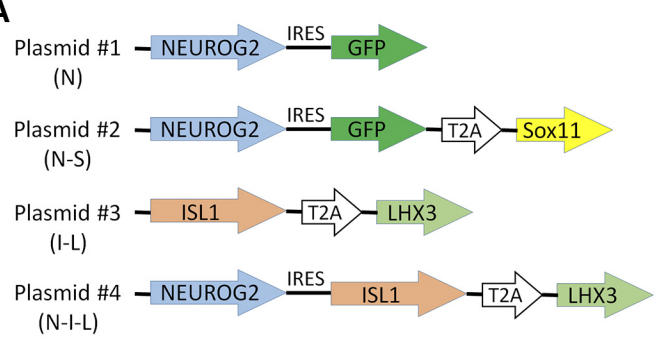

B

Factor name	Gene ID	Roles in MN differentiation
NEUROG2	63973	A neural-specific transcription factor that can specify a neuronal fate and is expressed in neural progenitor cells within the developing central and peripheral nervous systems.
Sox11	20666	A transcription factor involves in the regulation of embryonic development and may function in the developing nervous system.
ISL1	3670	A member of the LIM/homeodomain family of transcription factors and it is required for motor neuron generation.
LHX3	8022	A transcription factor that is required for motor neuron specification.

Fig. 2. Strategies to generate human induced pluripotent stem cell (iPSC)-derived motor neurons (MNs; iPSC-MNs) via lentiviral delivery of transcription factors. *A*: schematic diagrams show various transcription factors expressed in different lentiviral vectors (9, 33, 51). GFP, green fluorescent protein; IRES, internal ribosome entry site; ISL1 (I), insulin gene enhancer 1 or ISL LIM/homeobox 1; LHX3 (L), LIM/homeobox 3; NEUROG2 (N), neurogenin-2; Sox11 (S), mouse sex-determining region Y (SRY)-box transcription factor 11. *B*: roles of transcription factors involved in MN differentiation (28, 34, 37, 43).

41). However, most of these spontaneously differentiated neurons are glutamatergic neurons (~75%); ~15% are GABAergic, and ~5% are dopaminergic (TH+). There are very rare (<1%) MNs (HB9+) and cholinergic neurons (ChAT+; Fig. 1*E*). Therefore, it is not feasible to obtain human MNs via spontaneous differentiation of iPSC-NPCs.

Strategies to generate highly pure human MNs via lentiviral delivery of transcription factors. Lentiviral delivery of transcription factors is an efficient way to generate human MNs from iPSC-NPCs (13, 51). As NPCs are very sensitive to lentivirus dosage, to obtain high-quality MNs through this method, preparation of high-quality lentiviruses and addition of the proper amount at transduction are critical. Too high virus dosage will cause cell death and lead to low yield. On the other hand, if the dosage is too low, the purity of MN will be sacrificed because NPCs may not be efficiently transduced with lentiviruses and will generate more non-MNs via spontaneous differentiation (Fig. 1, *D* and *E*).

In our previous study, we successfully generated iPSC-MNs via lentiviral delivery of transcription factors (13, 51). In this method, NPCs are infected with two lentiviruses expressing four factors (N-S-I-L, the cocktail of *lentiviruses 2* and *3*; Fig. 2*A*). These factors play critical roles in either neuron differentiation or MN generation and specification (Fig. 2*B*). However, we noted some variations in MN purity, survival, and yield among different sets of experiments. Besides the impact of lentivirus quality, another factor that affects the MN outcomes could be the cotransduction of two lentiviruses. Some NPCs may not be simultaneously infected with both of these viruses, and thus they cannot be successfully induced into the MN subtype, leading to variations in MN purity in different preparations. A higher dosage of viruses will increase the transduction efficiency, but it will also cause more cell death and result in a low yield of mature MNs. Therefore, to generate highly pure MNs with high yield, we need to minimize the virus dosage to infect NPCs and meanwhile need to ensure that most NPCs are infected with virus and transcription factors are sufficiently expressed.

To this end, we have optimized the induction strategies with different combinations of transcription factors. Among our four previously used factors (N-S-I-L; 13, 51), Sox11 plays a general role in the development of the nervous system (Fig. 2*B*), and it is critical for direct conversion of MNs from fibroblasts (9, 33, 51). Given that NPCs are already of neuronal lineage, Sox11 may not be required for the generation of MNs from NPCs. If this is the case, a single virus expressing three factors (N-I-L) could be sufficient to induce iPSC-MNs and may significantly improve the MN purity and yield. Thus, we constructed a lentiviral vector in which three factors were simultaneously expressed (N-I-L, *plasmid 4*; Fig. 2*A*). As controls, other combinations of lentiviral vectors were also included in this study (Fig. 2*A*). We systematically examined and compared the induction of iPSC-MNs using three different combinations of factors: *1*) NEUROG2 alone (N, *lentivirus 1*);

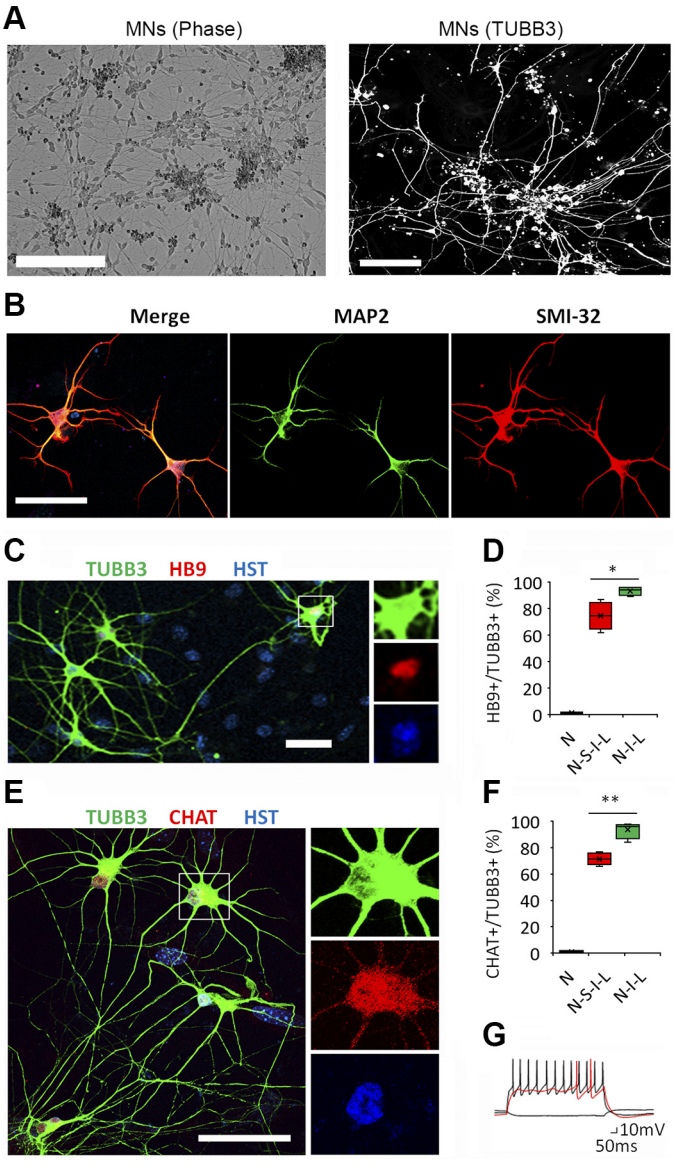

Fig. 3. Verification of motor neuron (MN) identity, purity, and maturation under different induction conditions. *A*: representative micrographs of induced pluripotent stem cell (iPSC)-derived MNs (iPSC-MNs) at 1 wk post-viral infection (WPI). *Left*: phase contrast. Scale bar, 200 μm. *Right*: immunostaining of tubulin β-3 class III (TUBB3). Scale bar, 100 μm. *B*: confocal micrographs of MNs at 1 WPI. Microtubule-associated protein 2 (MAP2) antibody recognizes dendrites, and neurofilament protein (SMI-32) antibody recognizes neurofilaments. Scale bar, 50 μm. *C*: confocal micrograph of MNs at 1.5 WPI. Neuronal marker TUBB3 shows the soma and neuron processes, Hoechst 33342 (HST) stained nuclei, and nuclear HB9 was used as the early MN marker. The MN highlighted with a rectangle is also shown at a high magnification with separated channels. Scale bar, 50 μm. *D*: quantification of MN fractions (HB9+/TUBB3+) under the indicated induction conditions. I, insulin gene enhancer 1 or ISL LIM/homeobox 1 (ISL1); L, LIM/homeobox 3 (LHX3); N, neurogenin-2 (NGN2); S, mouse sex-determining region Y (SRY)-box transcription factor 11 (Sox11). Number of neurons $n = 493$ for N, 407 for N-S-I-L, and 462 for N-I-L from 4 biological replicates. Student's *t* test was used for statistical analysis (N-S-I-L vs. N-I-L). $*P < 0.05$. *E*: confocal micrograph of MNs at 2 WPI. Neuronal marker TUBB3 shows the soma and neuron processes, HST stained nuclei, and choline acetyltransferase (ChAT) was used as a mature MN marker. The MN highlighted with a rectangle is also shown at a high magnification with separated channels. Scale bar, 50 μm. *F*: quantification of MN fractions (ChAT+/TUBB3+) under the indicated induction conditions. Number of neurons $n = 465$ for N, 412 for N-S-I-L, and 436 for N-I-L from 4 biological replicates. Student's *t* test was used for statistical analysis (N-S-I-L vs. N-I-L). $**P < 0.01$. *G*: repetitive action potential (AP) waveforms recorded under current-clamp mode of iPSC-MNs at 3 WPI. The precondition sweep and the sweep immediately above threshold (in red) are also shown.

2) NEUROG2, ISL1, LHX3, and Sox11 (N-S-I-L, the cocktail of *lentiviruses 2* and *3*); and *3*) NEUROG2, ISL1, and LHX3 (N-I-L, *lentivirus 4*; Fig. 2*A*).

Verification of MN identity and maturation. NPCs were cultured on Matrigel-coated six-well plates. When the cellular confluence was ~50% (Fig. 1*C*), proper amounts of lentiviruses were added at MOI of ~2 to infect NPCs. Within 1 WPI, neurites rapidly grew out from the soma, and cells became MN-like with very long axons (Fig. 3*A*). Immunostaining indicated that these induced neurons highly expressed generic neuron markers including TUBB3 (Fig. 3*A*), MAP2, and neurofilament protein (SMI-32; Fig. 3*B*). The highly expressed HB9 in nuclei (Fig. 3*C*) and the ChAT in the soma (Fig. 3*E*) verified that these induced neurons were of MN identity. We quantified the MN numbers among neuronal populations under different induction conditions. As expected, very few HB9+ neurons and ChAT+ neurons can be identified in the group of NEUROG2 alone (N). Excitingly, induction with a single virus expressing three factors (N-I-L) showed significantly higher MN fractions than the combination of four factors (N-S-I-L; Fig. 3, *D* and *F*). These results indicate that Sox11 is dispensable in the generation of MNs from NPCs. A single virus expressing three factors is sufficient to induce MNs and even gives rise to a higher purity.

To verify MN electrophysiological maturation, action potentials (APs) were recorded using a whole cell patch-clamp. Repetitive AP waveforms can be easily recorded under current-clamp of iPSC-MNs at 3 WPI (Fig. 3*G*). These results strongly support the idea that mature and functional human MNs can be obtained from iPSC-derived NPCs via lentiviral delivery of three transcription factors (N-I-L).

Optimized condition significantly improved the survival and yield of iPSC-MNs. Next, we examined and compared the survival and yield of iPSC-MNs that were induced under two different conditions. A surviving neuron was defined by two criteria: *1*) TUBB3 immunostaining shows typical neuronal morphology without obvious degeneration, and *2*) the soma contains a clear nucleus with HST staining (Fig. 3, *C* and *E*). Excitingly, the ratios of surviving neurons under the optimized condition (N-I-L) were higher than with the previous method (N-S-I-L), increased about 2-fold and 2.3-fold at 2 and 3 WPI, respectively (Fig. 4, *A* and *B*). Similarly, we quantified surviving neurons at 3 WPI and calculated the final yield with normalization to the starting materials. Strikingly, the yield of iPSC-MNs under the optimized condition was ~3 times that of the previous method (Fig. 4, *C* and *D*). These results demonstrate that the optimized condition using a single lentivirus expressing three factors dramatically improves the survival and the yield of iPSC-MNs.

DISCUSSION

Generation of neurons from hiPSCs greatly facilitates studies in understanding the regulatory mechanisms of neuronal development, determining the pathogenesis of neurological diseases, identifying molecular targets for therapeutic interventions, and screening drugs in a more human neuron-specific manner (15, 24, 29, 35, 36, 54). To achieve more reliable and disease-relevant findings, at least the following criteria should be considered to evaluate the cellular system in modeling human neurological diseases. First, the specific neuronal subtype that is particularly affected in the disease should be used in the research. For example, patient-derived MNs are the best neuronal subtype in modeling neurological diseases that target MNs. Second, neurons are able to achieve functional maturation. Some disease-related phenotypes may not be noticed until the diseased neurons reach the late mature stages, especially for modeling aging-dependent neurodegenerative diseases. Synaptic proteins, neurotransmitter-related enzymes, and electrophysiological activities are good measures to examine the

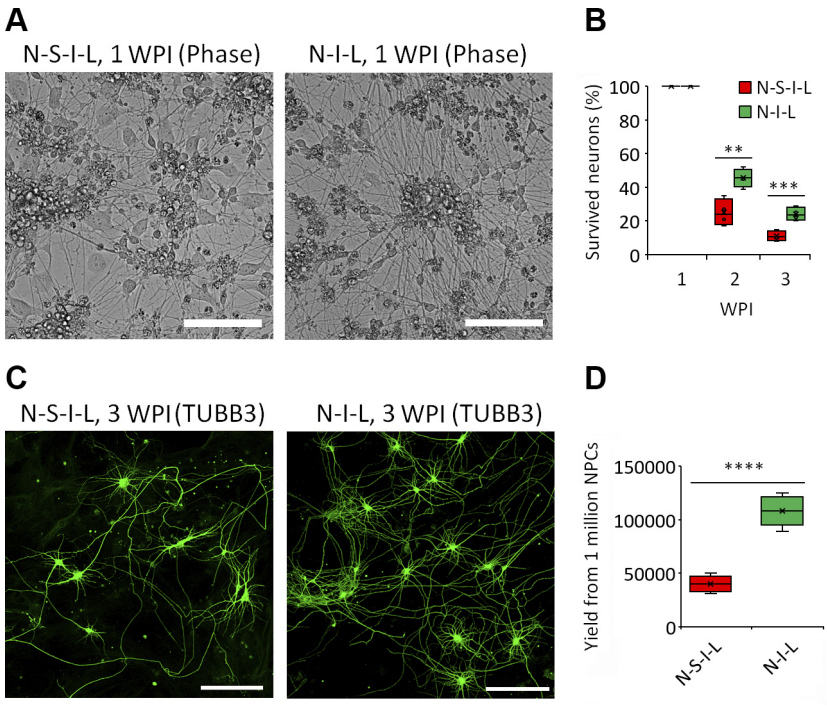

Fig. 4. Optimized induction condition dramatically improved induced pluripotent stem cell (iPSC)-derived motor neuron (MN; iPSC-MN) survival and yield. *A*: phase contrast micrographs of iPSC-MNs induced via the indicated combinations of transcription factors at 1 wk post-viral infection (WPI). Scale bars, 100 μm. *B*: surviving neurons under the indicated conditions. The number of neurons at 1 WPI was set as 100%. I, insulin gene enhancer 1 or ISL LIM/homeobox 1 (ISL1); L, LIM/homeobox 3 (LHX3); N, neurogenin-2 (NGN2); S, mouse sex-determining region Y (SRY)-box transcription factor 11 (Sox11). Number of neurons $n > 3{,}000$ from 4 biological replicates. Student's t test was used for statistical analysis (N-S-I-L vs. N-I-L). $^{**}P < 0.01$; $^{***}P < 0.001$. *C*: representative micrographs of iPSC-MNs induced via the indicated transcription factors at 3 WPI with immunostaining of tubulin β-3 class III (TUBB3). Scale bars, 100 μm. *D*: yield of iPSC-MNs at 3 WPI from 1 million neuronal progenitor cells (NPCs) at transduction. The results represent 4 biological replicates. Student's t test was used for statistical analysis. $^{****}P < 0.0001$.

maturation and functions. Third, the purity and the yield should be good enough for analysis. Generally, immunostaining of specific markers could be able to distinguish the target neurons from other types of cocultured cells. However, to biochemically identify dysregulated factors in diseased neurons, large amounts of specific neurons with very high purity are required. Finally, culture the neurons more physiologically and maximize the relevance to in vivo conditions. Using extracellular matrix (ECM) protein coated culture vessels and culture medium supplemented with neurotrophic factors, and coculture of neurons and glial cells could be necessary to make the neuronal culture more physiological and improve the survival.

In this study, using the lentiviral delivery of transcription factors, we have successfully generated functional human MNs from iPSCs and further optimized the induction conditions. This optimized approach minimized the virus dosage by switching two viruses expressing four factors to a single virus expressing three factors and thus significantly improved the neuronal survival and gave rise to high yield and purity. This approach makes it feasible to obtain abundant materials for biochemical studies in determining the pathogenesis of MN-related diseases.

As noninfected cells will spontaneously differentiate into non-MNs, generation of higher-purity MNs requires higher transduction efficiency. Thus, the preparation of high-quality lentivirus is very important to achieve good infection efficiency (>95%). On the other hand, a higher dosage of virus will cause more cell death and lead to low yield. In our practice, we routinely test the titer of active virus in each preparation (12) and use a proper virus dosage to infect NPCs. Thereby the transduction efficiency and neuron survival could be well balanced based on active virus titer. In this study, a single virus was used to coexpress essential and sufficient factors to generate MNs, and thus we can maximize the transduction efficiency and minimize cell death, obtaining highly pure iPSC-MNs with high yield.

Compared with other approaches, iPSC-MNs induced by lentiviral delivery of transcription factors possess unique features, such as high purity (>90%) and fully functional maturity. These neurons robustly express MN marker HB9, ISL1, and ChAT and mature neuron markers MAP2 and presynaptic proteins and show electrical maturation and firing of action potentials within 3 wk (13, 51). These unique features make such iPSC-MNs an excellent research system in modeling movement disorders in vitro. Most importantly, in this study we further optimized the induction conditions and significantly improved survival and yield, making it feasible to obtain a large amount of functional mature iPSC-MNs.

Generation of abundant and highly pure MNs from patient-specific iPSCs is the prerequisite for biochemically determining the pathogenesis of movement disorders and identifying molecular targets for therapeutic interventions. For example, genome-wide analysis of gene expression using RNA-sequencing (RNAseq) techniques and determining the transcriptional and epigenetic regulations of gene expression using chromatin immunoprecipitation (ChIP; 10, 11, 14, 39, 44). Additionally, using patient-derived neurons, studies in RNA-protein interactions could reveal the regulation and dysregulation of RNA metabolism, and Co-IP-MS analysis could identify dysregulated factors in diseased neurons (32, 45). All these biochemical approaches require large amounts of pure materials.

Another big challenge in modeling neurological diseases using iPSC-derived neurons is how to culture the neurons more physiologically, especially for long-term culture. Chemical or physical modifications of the cell culture plates, such as coating with ECM proteins, have been demonstrated to be an efficient method to better mimic in vivo cell behavior (26). In some studies, neuroglial coculture is required for modeling certain diseases, for exploring neuroglial interactions, and for a long-term survival (27, 38, 50). In this study, we cultured iPSCs, NPCs, and MNs on Matrigel-coated plates. For long-term cultures (>2 wk), iPSC-MNs were seeded onto culture plates coated with a monolayer of astrocytes. These measures make the culture more physiological and maximize the relevance to in vivo conditions.

ACKNOWLEDGMENTS

We thank members of the Ding laboratory and Dr. Chun-Li Zhang (University of Texas Southwestern Medical Center) for help and discussion.

GRANTS

This work was supported by NIH Grant R21NS112910 to B.D. and Department of Defense Peer Reviewed Medical Research Program Grant W81XWH2010186 to B.D.

DISCLOSURES

No conflicts of interest, financial or otherwise, are declared by the authors.

AUTHOR CONTRIBUTIONS

B.D. conceived and designed research; M.S. and B.D. performed experiments; M.S. and B.D. analyzed data; M.S. and B.D. interpreted results of experiments; B.D. prepared figures; M.S. and B.D. drafted manuscript; M.S. and B.D. edited and revised manuscript; M.S. and B.D. approved final version of manuscript.

REFERENCES

1. **Arber S, Han B, Mendelsohn M, Smith M, Jessell TM, Sockanathan S.** Requirement for the homeobox gene *Hb9* in the consolidation of motor neuron identity. *Neuron* 23: 659–674, 1999. doi:10.1016/S0896-6273(01)80026-X.
2. **Bally-Cuif L, Hammerschmidt M.** Induction and patterning of neuronal development, and its connection to cell cycle control. *Curr Opin Neurobiol* 13: 16–25, 2003. doi:10.1016/S0959-4388(03)00015-1.
3. **Ben-Shushan E, Feldman E, Reubinoff BE.** Notch signaling regulates motor neuron differentiation of human embryonic stem cells. *Stem Cells* 33: 403–415, 2015. doi:10.1002/stem.1873.
4. **Bianchi F, Malboubi M, Li Y, George JH, Jerusalem A, Szele F, Thompson MS, Ye H.** Rapid and efficient differentiation of functional motor neurons from human iPSC for neural injury modelling. *Stem Cell Res (Amst)* 32: 126–134, 2018. doi:10.1016/j.scr.2018.09.006.
5. **Busskamp V, Lewis NE, Guye P, Ng AH, Shipman SL, Byrne SM, Sanjana NE, Murn J, Li Y, Li S, Stadler M, Weiss R, Church GM.** Rapid neurogenesis through transcriptional activation in human stem cells. *Mol Syst Biol* 10: 760, 2014. doi:10.15252/msb.20145508.
6. **Cave C, Sockanathan S.** Transcription factor mechanisms guiding motor neuron differentiation and diversification. *Curr Opin Neurobiol* 53: 1–7, 2018. doi:10.1016/j.conb.2018.04.012.
7. **Chambers SM, Fasano CA, Papapetrou EP, Tomishima M, Sadelain M, Studer L.** Highly efficient neural conversion of human ES and iPS cells by dual inhibition of SMAD signaling. *Nat Biotechnol* 27: 275–280, 2009 [Erratum in *Nat Biotechnol* 27: 485, 2009]. doi:10.1038/nbt.1529.
8. **Ding B.** Gene expression in maturing neurons: regulatory mechanisms and related neurodevelopmental disorders. *Sheng Li Xue Bao* 67: 113–133, 2015.
9. **Ding B, Akter M, Zhang CL.** Differential influence of sample sex and neuronal maturation on mRNA and protein transport in induced human neurons. *Front Mol Neurosci* 13: 46, 2020. doi:10.3389/fnmol.2020.00046.

10. **Ding B, Cave JW, Dobner PR, Mullikin-Kilpatrick D, Bartzokis M, Zhu H, Chow CW, Gronostajski RM, Kilpatrick DL.** Reciprocal autoregulation by NFI occupancy and ETV1 promotes the developmental expression of dendrite-synapse genes in cerebellar granule neurons. *Mol Biol Cell* 27: 1488–1499, 2016. doi:10.1091/mbc.E15-07-0476.
11. **Ding B, Dobner PR, Mullikin-Kilpatrick D, Wang W, Zhu H, Chow CW, Cave JW, Gronostajski RM, Kilpatrick DL.** BDNF activates an NFI-dependent neurodevelopmental timing program by sequestering NFATc4. *Mol Biol Cell* 29: 975–987, 2018. doi:10.1091/mbc.E16-08-0595.
12. **Ding B, Kilpatrick DL.** Lentiviral vector production, titration, and transduction of primary neurons. *Methods Mol Biol* 1018: 119–131, 2013. doi:10.1007/978-1-62703-444-9_12.
13. **Ding B, Tang Y, Ma S, Akter M, Liu ML, Zang T, Zhang CL.** Disease modeling with human neurons reveals LMNB1 dysregulation underlying DYT1 dystonia (Preprint). *bioRxiv* 2020. doi:10.1101/2020.08.11.246371.
14. **Ding B, Wang W, Selvakumar T, Xi HS, Zhu H, Chow CW, Horton JD, Gronostajski RM, Kilpatrick DL.** Temporal regulation of nuclear factor one occupancy by calcineurin/NFAT governs a voltage-sensitive developmental switch in late maturing neurons. *J Neurosci* 33: 2860–2872, 2013. doi:10.1523/JNEUROSCI.3533-12.2013.
15. **Engle SJ, Blaha L, Kleiman RJ.** Best practices for translational disease modeling using human iPSC-derived neurons. *Neuron* 100: 783–797, 2018. doi:10.1016/j.neuron.2018.10.033.
16. **Fisher KM, Zaaimi B, Williams TL, Baker SN, Baker MR.** Beta-band intermuscular coherence: a novel biomarker of upper motor neuron dysfunction in motor neuron disease. *Brain* 135: 2849–2864, 2012. doi:10.1093/brain/aws150.
17. **Fujimori K, Ishikawa M, Otomo A, Atsuta N, Nakamura R, Akiyama T, Hadano S, Aoki M, Saya H, Sobue G, Okano H.** Modeling sporadic ALS in iPSC-derived motor neurons identifies a potential therapeutic agent. *Nat Med* 24: 1579–1589, 2018. doi:10.1038/s41591-018-0140-5.
18. **Gascón S, Masserdotti G, Russo GL, Götz M.** Direct neuronal reprogramming: achievements, hurdles, and new roads to success. *Cell Stem Cell* 21: 18–34, 2017. doi:10.1016/j.stem.2017.06.011.
19. **Goparaju SK, Kohda K, Ibata K, Soma A, Nakatake Y, Akiyama T, Wakabayashi S, Matsushita M, Sakota M, Kimura H, Yuzaki M, Ko SB, Ko MS.** Rapid differentiation of human pluripotent stem cells into functional neurons by mRNAs encoding transcription factors. *Sci Rep* 7: 42367, 2017. doi:10.1038/srep42367.
20. **Guo W, Naujock M, Fumagalli L, Vandoorne T, Baatsen P, Boon R, Ordovás L, Patel A, Welters M, Vanwelden T, Geens N, Tricot T, Benoy V, Steyaert J, Lefebvre-Omar C, Boesmans W, Jarpe M, Sterneckert J, Wegner F, Petri S, Bohl D, Vanden Berghe P, Robberecht W, Van Damme P, Verfaillie C, Van Den Bosch L.** HDAC6 inhibition reverses axonal transport defects in motor neurons derived from FUS-ALS patients. *Nat Commun* 8: 861, 2017. doi:10.1038/s41467-017-00911-y.
21. **Hall CE, Yao Z, Choi M, Tyzack GE, Serio A, Luisier R, Harley J, Preza E, Arber C, Crisp SJ, Watson PM, Kullmann DM, Abramov AY, Wray S, Burley R, Loh SH, Martins LM, Stevens MM, Luscombe NM, Sibley CR, Lakatos A, Ule J, Gandhi S, Patani R.** Progressive motor neuron pathology and the role of astrocytes in a human stem cell model of VCP-related ALS. *Cell Rep* 19: 1739–1749, 2017. doi:10.1016/j.celrep.2017.05.024.
22. **Hu BY, Weick JP, Yu J, Ma LX, Zhang XQ, Thomson JA, Zhang SC.** Neural differentiation of human induced pluripotent stem cells follows developmental principles but with variable potency. *Proc Natl Acad Sci USA* 107: 4335–4340, 2010. doi:10.1073/pnas.0910012107.
23. **Kanning KC, Kaplan A, Henderson CE.** Motor neuron diversity in development and disease. *Annu Rev Neurosci* 33: 409–440, 2010. doi:10.1146/annurev.neuro.051508.135722.
24. **Karagiannis P, Takahashi K, Saito M, Yoshida Y, Okita K, Watanabe A, Inoue H, Yamashita JK, Todani M, Nakagawa M, Osawa M, Yashiro Y, Yamanaka S, Osafune K.** Induced pluripotent stem cells and their use in human models of disease and development. *Physiol Rev* 99: 79–114, 2019. doi:10.1152/physrev.00039.2017.
25. **Kiskinis E, Kralj JM, Zou P, Weinstein EN, Zhang H, Tsioras K, Wiskow O, Ortega JA, Eggan K, Cohen AE.** All-optical electrophysiology for high-throughput functional characterization of a human iPSC-derived motor neuron model of ALS. *Stem Cell Reports* 10: 1991–2004, 2018. doi:10.1016/j.stemcr.2018.04.020.
26. **Lam D, Enright HA, Cadena J, Peters SK, Sales AP, Osburn JJ, Soscia DA, Kulp KS, Wheeler EK, Fischer NO.** Tissue-specific extracellular matrix accelerates the formation of neural networks and communities in a neuron-glia co-culture on a multi-electrode array. *Sci Rep* 9: 4159, 2019. doi:10.1038/s41598-019-40128-1.
27. **Le Berre-Scoul C, Chevalier J, Oleynikova E, Cossais F, Talon S, Neunlist M, Boudin H.** A novel enteric neuron-glia coculture system reveals the role of glia in neuronal development. *J Physiol* 595: 583–598, 2017. doi:10.1113/JP271989.
28. **Lee S, Cuvillier JM, Lee B, Shen R, Lee JW, Lee SK.** Fusion protein Isl1-Lhx3 specifies motor neuron fate by inducing motor neuron genes and concomitantly suppressing the interneuron programs. *Proc Natl Acad Sci USA* 109: 3383–3388, 2012. doi:10.1073/pnas.1114515109.
29. **Lee S, Huang EJ.** Modeling ALS and FTD with iPSC-derived neurons. *Brain Res* 1656: 88–97, 2017. doi:10.1016/j.brainres.2015.10.003.
30. **Liewluck T, Saperstein DS.** Progressive muscular atrophy. *Neurol Clin* 33: 761–773, 2015. doi:10.1016/j.ncl.2015.07.005.
31. **Lin X, Li JJ, Qian WJ, Zhang QJ, Wang ZF, Lu YQ, Dong EL, He J, Wang N, Ma LX, Chen WJ.** Modeling the differential phenotypes of spinal muscular atrophy with high-yield generation of motor neurons from human induced pluripotent stem cells. *Oncotarget* 8: 42030–42042, 2017. doi:10.18632/oncotarget.14925.
32. **Lindoso RS, Kasai-Brunswick TH, Monnerat Cahli G, Collino F, Bastos Carvalho A, Campos de Carvalho AC, Vieyra A.** Proteomics in the world of induced pluripotent stem cells. *Cells* 8: 703, 2019. doi:10.3390/cells8070703.
33. **Liu ML, Zang T, Zhang CL.** Direct lineage reprogramming reveals disease-specific phenotypes of motor neurons from human ALS patients. *Cell Reports* 14: 115–128, 2016. doi:10.1016/j.celrep.2015.12.018.
34. **Ma YC, Song MR, Park JP, Ho HY, Hu L, Kurtev MV, Zieg J, Ma Q, Pfaff SL, Greenberg ME.** Regulation of motor neuron specification by phosphorylation of neurogenin 2. *Neuron* 58: 65–77, 2008. doi:10.1016/j.neuron.2008.01.037.
35. **Maury Y, Côme J, Piskorowski RA, Salah-Mohellibi N, Chevaleyre V, Peschanski M, Martinat C, Nedelec S.** Combinatorial analysis of developmental cues efficiently converts human pluripotent stem cells into multiple neuronal subtypes. *Nat Biotechnol* 33: 89–96, 2015. doi:10.1038/nbt.3049.
36. **Mertens J, Reid D, Lau S, Kim Y, Gage FH.** Aging in a dish: iPSC-derived and directly induced neurons for studying brain aging and age-related neurodegenerative diseases. *Annu Rev Genet* 52: 271–293, 2018. doi:10.1146/annurev-genet-120417-031534.
37. **Moore DL, Goldberg JL.** Multiple transcription factor families regulate axon growth and regeneration. *Dev Neurobiol* 71: 1186–1211, 2011. doi:10.1002/dneu.20934.
38. **Nadadhur AG, Alsaqati M, Gasparotto L, Cornelissen-Steijger P, van Hugte E, Dooves S, Harwood AJ, Heine VM.** Neuron-glia interactions increase neuronal phenotypes in tuberous sclerosis complex patient iPSC-derived models. *Stem Cell Reports* 12: 42–56, 2019. doi:10.1016/j.stemcr.2018.11.019.
39. **Ng SY, Soh BS, Rodriguez-Muela N, Hendrickson DG, Price F, Rinn JL, Rubin LL.** Genome-wide RNA-Seq of human motor neurons implicates selective ER stress activation in spinal muscular atrophy. *Cell Stem Cell* 17: 569–584, 2015. doi:10.1016/j.stem.2015.08.003.
40. **Patani R.** Generating diverse spinal motor neuron subtypes from human pluripotent stem cells. *Stem Cells Int* 2016: 1036974, 2016. doi:10.1155/2016/1036974.
41. **Phillis JW.** Acetylcholine release from the central nervous system: a 50-year retrospective. *Crit Rev Neurobiol* 17: 161–217, 2005. doi:10.1615/CritRevNeurobiol.v17.i3-4.30.
42. **Ragagnin AM, Shadfar S, Vidal M, Jamali MS, Atkin JD.** Motor neuron susceptibility in ALS/FTD. *Front Neurosci* 13: 532, 2019. doi:10.3389/fnins.2019.00532.
43. **Rhee HS, Closser M, Guo Y, Bashkirova EV, Tan GC, Gifford DK, Wichterle H.** Expression of terminal effector genes in mammalian neurons is maintained by a dynamic relay of transient enhancers. *Neuron* 92: 1252–1265, 2016. doi:10.1016/j.neuron.2016.11.037.
44. **Rizzo F, Ramirez A, Compagnucci C, Salani S, Melzi V, Bordoni A, Fortunato F, Niceforo A, Bresolin N, Comi GP, Bertini E, Nizzardo M, Corti S.** Genome-wide RNA-seq of iPSC-derived motor neurons indicates selective cytoskeletal perturbation in Brown-Vialetto disease that is partially rescued by riboflavin. *Sci Rep* 7: 46271, 2017. doi:10.1038/srep46271.
45. **Sances S, Bruijn LI, Chandran S, Eggan K, Ho R, Klim JR, Livesey MR, Lowry E, Macklis JD, Rushton D, Sadegh C, Sareen D, Wichterle H, Zhang SC, Svendsen CN.** Modeling ALS with motor neurons derived

from human induced pluripotent stem cells. *Nat Neurosci* 19: 542–553, 2016. doi:10.1038/nn.4273.

46. **Sareen D, O'Rourke JG, Meera P, Muhammad AK, Grant S, Simpkinson M, Bell S, Carmona S, Ornelas L, Sahabian A, Gendron T, Petrucelli L, Baughn M, Ravits J, Harms MB, Rigo F, Bennett CF, Otis TS, Svendsen CN, Baloh RH.** Targeting RNA foci in iPSC-derived motor neurons from ALS patients with a *C9ORF72* repeat expansion. *Sci Transl Med* 5: 208ra149, 2013. doi:10.1126/scitranslmed.3007529.
47. **Schildge S, Bohrer C, Beck K, Schachtrup C.** Isolation and culture of mouse cortical astrocytes. *J Vis Exp* (71): 50079, 2013. doi:10.3791/50079.
48. **Shimojo D, Onodera K, Doi-Torii Y, Ishihara Y, Hattori C, Miwa Y, Tanaka S, Okada R, Ohyama M, Shoji M, Nakanishi A, Doyu M, Okano H, Okada Y.** Rapid, efficient, and simple motor neuron differentiation from human pluripotent stem cells. *Mol Brain* 8: 79, 2015. doi:10.1186/s13041-015-0172-4.
49. **Singh VK, Kalsan M, Kumar N, Saini A, Chandra R.** Induced pluripotent stem cells: applications in regenerative medicine, disease modeling, and drug discovery. *Front Cell Dev Biol* 3: 2, 2015. doi:10.3389/fcell.2015.00002.
50. **Swire M, Ffrench-Constant C.** Oligodendrocyte-neuron myelinating coculture. In: *Oligodendrocytes*, edited by Lyons DA, Kegel L. New York: Springer, 2019, p. 111–128. doi:10.1007/978-1-4939-9072-6_7.
51. **Tang Y, Liu ML, Zang T, Zhang CL.** Direct reprogramming rather than iPSC-based reprogramming maintains aging hallmarks in human motor neurons. *Front Mol Neurosci* 10: 359, 2017. doi:10.3389/fnmol.2017.00359.
52. **Verber NS, Shepheard SR, Sassani M, McDonough HE, Moore SA, Alix JJ, Wilkinson ID, Jenkins TM, Shaw PJ.** Biomarkers in motor neuron disease: a state of the art review. *Front Neurol* 10: 291, 2019. doi:10.3389/fneur.2019.00291.
53. **Wu C, Watts ME, Rubin LL.** MAP4K4 activation mediates motor neuron degeneration in amyotrophic lateral sclerosis. *Cell Rep* 26: 1143–1156.e5, 2019. doi:10.1016/j.celrep.2019.01.019.
54. **Wu YY, Chiu FL, Yeh CS, Kuo HC.** Opportunities and challenges for the use of induced pluripotent stem cells in modelling neurodegenerative disease. *Open Biol* 9: 180177, 2019. doi:10.1098/rsob.180177.
55. **Yamanaka S, Takahashi K.** [Induction of pluripotent stem cells from mouse fibroblast cultures]. *Tanpakushitsu kakusan koso* 51: 2346–2351, 2006.
56. **Yang J, Tang Y, Liu H, Guo F, Ni J, Le W.** Suppression of histone deacetylation promotes the differentiation of human pluripotent stem cells towards neural progenitor cells. *BMC Biol* 12: 95, 2014. doi:10.1186/s12915-014-0095-z.
57. **Zomer HD, Vidane AS, Gonçalves NN, Ambrósio CE.** Mesenchymal and induced pluripotent stem cells: general insights and clinical perspectives. *Stem Cells Cloning* 8: 125–134, 2015. doi:10.2147/SCCAA.S88036.